Available online at http://scik.org
Commun. Math. Biol. Neurosci. 2024, 2024:117
https://doi.org/10.28919/cmbn/8741
ISSN: 2052-2541

EPIDEMIOLOGY SIMULATION: NUMERICAL TECHNIQUES FOR ANALYZING TYPE 2 DIABETES MODEL AND ITS PREVENTION MEASURES

N. JEEVA[1,*], K.M. DHARMALINGAM[1], NASIR ALI[2,*], MOHAMED Z. SAYED-AHMED[3], REDA M. RADWAN[4], HESHAM S. EL-BAHKIRY[4], SUNDAY EMMANUEL FADUGBA[5], KAYODE OSHINUBI[6], KEKANA MALESELA[7], ADEJIMI ADENIJI[7], FIKADU TESGERA TOLASA[8]

[1]PG and Research Department of Mathematics, The Madura College, Madurai, Tamil Nadu, India
[2]COMSATS University Islamabad, Vehari Campus, 61100, Vehari, Pakistan
[3]Department of Clinical Practice, College of Pharmacy, Jazan University, Jazan, 45142, Saudi Arabia
[4]Department of Diagnostic Radiography Technology, College of Nursing and Health Sciences, Jazan University, Jazan, 45142, Saudi Arabia
[5]Department of Mathematics, Ekiti State University, Ado Ekiti, 360001, Nigeria
[6]School of Informatics, Computing and Cyber Systems, Northern Arizona University, Flagstaff, AZ 86011, USA
[7]Department of Mathematics and Statistics, Tshwane University of Technology, Pretoria, South Africa
[8]Department of Mathematics, Dambidollo University, Dambidollo, Oromia, Ethiopia

Abstract. Type 2 diabetes (T2D) is a chronic illness that affects how well the body uses glucose, an essential energy source. Individuals with type 2 diabetes do not produce enough insulin or do not respond to control blood sugar levels. Clinical trials have suggested that poor nutritional habits may contribute to an increase in the incidence of type 2 diabetes. We investigated the dynamics of type 2 diabetes mellitus (T2D), which was formulated based on an epidemic mathematical model. The model categorizes the population into five compartments: Susceptible $S(t)$, Affected $A(t)$, Treated $T(t)$, Healthy Lifestyle $L(t)$, and Prevented $P(t)$ individuals. We used the Homotopy Analysis Method (HAM) and Homotopy Perturbation Method (HPM) to provide a thorough analytical study of

*Corresponding authors
E-mail addresses: jeevapirc2405@gmail.com, nasirzawar@gmail.com
Received July 02, 2024

this distinct model. To confirm the region of convergence in the HAM solutions for our model, the h-curves are provided. MATLAB coding was used for comparison with HAM and HPM to verify the accuracy and efficacy of the obtained solutions. We noticed no substantial difference between the analytical and numerical results. Moreover, in order to examine the behavior of the model individuals, we varied each parameter. Through this analysis, we obtained valuable insights into the responses of the type 2 diabetes model under various conditions and scenarios. This research offers valuable insights into the utilization of semi-analytical methods for analyzing epidemiological models related to infectious diseases, providing significant utility for researchers in the field.

Keywords: type 2 diabetes (T2D); epidemic mathematical model; numerical analysis; homotopy analysis method (HAM); homotopy perturbation method (HPM); h-curves.

2020 AMS Subject Classification: 34A34, 34E10, 65L06.

1. INTRODUCTION

High blood sugar levels are a defining indicators of type 2 diabetes, which is a chronic metabolic illness. Genetic factors, lack of physical activity, unhealthy diet, obesity, and aging are risk factors. Unlike type 1 diabetes, which often manifests in childhood, type 2 diabetes is associated with insulin resistance, and typically develops later in life. Increased thirst, frequent urination, weight loss, exhaustion, and visual issues are some of these symptoms. Changes in lifestyle, medicine, or insulin treatment are all part of management. If left untreated, type 2 diabetes can lead to damage to the kidneys and heart failure, highlighting the significance of regular monitoring and a healthy lifestyle [1]–[4].

The prevalence of type 2 diabetes worldwide, need for early identification and prevention, requirement for individualized care, and possible advantages of continuous glucose monitoring systems. [5] provides estimates of the global incidence of diabetes for 2019, as well as projections for 2030 and 2045, highlighting the greater incidence in high-income countries and metropolitan regions. A significant proportion of people with diabetes are oblivious to their illness, and comprehensive estimates for various geographic areas and socioeconomic classes indicate that the number of people with diabetes may increase if timely measures are not implemented. A person with diabetes has a twofold higher chance of developing different vascular illnesses. The relationship between fasting blood glucose concentration and vascular risk is nonlinear, and in individuals without a history of diabetes, the addition of information about multiple conventional risk factors to that about fasting blood glucose level or poor fasting glucose status

does not significantly enhance the prediction of vascular disease. The need to identify gender and sex variations in the different elements of type 2 diabetes mellitus (T2DM) is pointed out, underscoring the necessity of customized therapy that takes into account variations in biology, genetics, hormones, and the environment. With an emphasis on sex-specific outcomes, special attention is given to the management of diabetes during pregnancy, highlighting its influence on progeny health. In addition to encouraging a deeper investigation of the underlying processes, the demand for comprehensive biomedical research seeks to address gender-based differences in the burden of T2DM throughout different life stages [6]–[9].

A strong negative link between type 2 diabetes risk and physical activity was found in a meta-analysis that focused on the role of decreased adiposity in mediating this association. With 5-7 hours of varied activities per week, there is a noticeable decrease in risk, indicating an ideal threshold for risk reduction [10].

Statistical modelling is a fundamental epidemiological framework used to visualize the spread of illnesses. Mathematical techniques are used to analyze and forecast the distribution and transmission of diseases within a population. The abbreviation ”SIR” is used to categorize individuals in the population into three categories: Susceptible, Infected, and Recovered. To provide a mathematical framework for comprehending these viruses, a number of models, such as those for COVID-19, Ebola, Zika, and other diseases, have been developed with modified versions of epidemiology. These models are essential for understanding, predicting, and planning disease management and prevention initiatives [11]–[16]. In alignment with this concept, the T2D model was structured as a SATLP epidemic model, which denotes Susceptible, Affected, Treated, Healthy Lifestyle, and Prevented individuals. This study explored the impact of lifestyle interventions on individuals through the development of an ordinary differential equation model. This study introduces a comprehensive model that integrates the dynamics of T2D by incorporating a control variable known as healthy lifestyle [17].

In scientific and technical applications, semi-analytical approaches play a crucial role in resolving intricate mathematical issues by providing a compromise between the numerical versatility and analytical accuracy. These approaches are useful, especially when nonlinearity or

system complexity makes analytical solutions difficult. Semi-analytical techniques offer a precise and effective method to solve practical issues in a range of domains by merging analytical expressions with numerical computations. A wide variety of semi-analytical methods, including the Differential Transform Method (DTM), Adomian Decomposition Method (ADM), Akbari Ganji's Method (AGM), Laplace Adomian Decomposition Method (LADM), Taylor Series Method (TSM), and Variation Iteration Method (VIM), have been used to address complex mathematical problems [18]–[29]. The Homotopy Analysis Method (HAM) and Homotopy Perturbation Method (HPM) are highly effective semi-analytical methods for solving nonlinear equations. These approaches provide accurate responses by combining analytical and numerical techniques, making them useful for solving a wide range of mathematics and engineering problems, owing to their versatility and efficacy [30]–[34].

This study aimed to provide semi-analytical solutions using HAM and HPM for a type 2 diabetes model. To examine the dynamics of the system and its preventive measures in T2D, parameter variations were performed. This paper is organized as follows: In Section 2, the mathematical model of type 2 diabetes is explained through an in-depth description of the governing equations. A numerical analysis (HAM and HPM) of the governing system of nonlinear differential equations is presented in Section 3. Section 4 presents the results of the numerical analysis (Figures and Tables) along with a discussion of the findings. Section 5 presents the conclusions of the study.

2. TYPE 2 DIABETES MODEL

In this study, we consider type 2 diabetes (T2D) model developed by Anika Ferdous [17]. The entire population of individuals aged 20 to 79, denoted as $N(t)$, is subsequently categorized into five classes. All adults are assumed to be potentially susceptible $S(t)$ and those in this category with healthy lifestyles are designated as $L(t)$. Affected adults are classified as $A(t)$, and once they start treatment, they are called $T(t)$. $P(t)$ is a category for those who have prevented or recovered from T2D. Thus, the system of ordinary differential equations of the type 2 diabetes (T2D) model is given as:

$$\frac{dS}{dt} = \Omega - (\eta + \theta + \kappa)S$$

$$
\begin{aligned}
\frac{dA}{dt} &= \theta S - (\sigma + \eta + \delta_1)A + \zeta L \\
\frac{dT}{dt} &= \sigma A - (\eta + \delta_2)T \\
\frac{dL}{dt} &= \kappa S - (\zeta + \eta + \phi)L \\
\frac{dP}{dt} &= \phi L - \eta P
\end{aligned} \tag{1}
$$

with the initial conditions:

$$S(0) = q_1, \;\; A(0) = q_2, \;\; T(0) = q_3 \;\; , L(0) = q_4 \;\; , P(0) = q_5 \tag{2}$$

where parameter η represents the natural mortality rate and Ω represents the birth rate. Parameters θ and ζ symbolize the diabetes rates from the susceptible and healthy lifestyle compartments, respectively. The parameter σ represents the treatment rate, whereas κ denotes the rate of susceptible adults maintaining a healthy lifestyle. Finally, ϕ represents the rate at which the healthy lifestyle population transitions to the prevented class. Adults can die from diabetes-related complications in classes A (t) and T (t) at the rates δ_1 and δ_2, respectively. Therefore, $A\delta_1 + T\delta_2$ can be used to compute the number of adult deaths from diabetes each year. Furthermore, given that the treated people in class T have a lower mortality rate than the afflicted persons in class A, it is anticipated that $\delta_2 < \delta_1$.

In the absence of an exact solution, we present semi-analytical solutions to Equation (1) using HAM and HPM. Both MATLAB and MAPLE were used to conduct a thorough and in-depth analysis of the model.

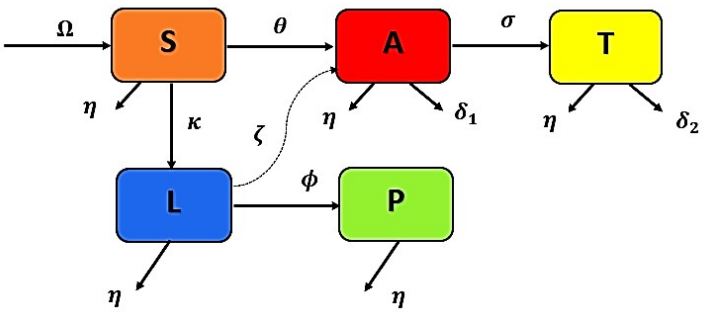

FIGURE 1. Flow chart of T2D model

TABLE 1. Parameters and values

Parameters	Values (unit: per year)	Source
Ω	0.621	[17]
η	0.0138	[17]
θ	0.142	[17]
ϕ	0.3	[17]
κ	0.2	[17]
σ	0.565	[17]
ζ	0.05	[17]
δ_1	0.04	[17]
δ_2	0.002	[17]

TABLE 2. Initial conditions are assumed at $t = 0$

Initial values	Values
$S(0)$	20
$A(0)$	10
$T(0)$	5
$L(0)$	5
$P(0)$	5

3. NUMERICAL TECHNIQUES FOR THE T2D MODEL

The Homotopy Analysis Method (HAM) and Homotopy Perturbation Method (HPM) are related techniques used for solving nonlinear differential equations. HPM and HAM are commonly used because they are simple and efficient in dealing with nonlinearities, especially when there is strong nonlinearity or singular aspects. These techniques generate semi-analytical solutions in the form of convergent series, which helps to understand the solution's behaviour. Both methods rely on constructing a homotopy; HAM aims to provide accurate approximations of the solution using the homotopy curve (h-curve), which serves as a visual depiction of the solution's convergence behavior. It attempts to improve the convergence region and rate by incorporating the auxiliary parameters. On the other hand, HPM uses a perturbation parameter p to iteratively improve the solution.

3.1. Homotopy Analysis Method (HAM). In this subsection, we apply HAM for the T2D model (1). To apply the HAM, we fix $S(0) = S_0(t) = q_1, A(0) = A_0(t) = q_2, T(0) = T_0(t) = q_3$, $L(0) = L_0(t) = q_4$, $P(0) = P_0(t) = q_5$, as initial approximation of $S(t)$, $A(t)$, $T(t)$, $L(t)$, and $P(t)$.

Let $\Psi \in [0,1]$ presumed as an embedding parameter. The continuous mappings for HAM can be defined as:

$$\begin{aligned} S(t) &\to \Phi_1(t;\Psi) \\ A(t) &\to \Phi_2(t;\Psi) \\ T(t) &\to \Phi_3(t;\Psi) \\ L(t) &\to \Phi_4(t;\Psi) \\ P(t) &\to \Phi_5(t;\Psi) \end{aligned} \tag{3}$$

In a way that rises with embedding parameter Ψ from 0 to 1, $\Phi(t;\Psi)$ differs from the initial iterations to exact findings. We choose linear operator as

$$L_i[\Phi_i(t;\Psi)] = \frac{\partial \Phi_i(t;\Psi)}{\partial t}, i = 1,2,3,4,5 \tag{4}$$

which satisfies $L_i[c_i]$, where c_i are integral constants. Now, the nonlinear operators are defined as follows:

$$\begin{aligned} N_1[\Phi_i(t;\Psi)] &= \frac{\partial \Phi_i(t;\Psi)}{\partial t} - \Omega + (\eta + \theta + \kappa)\Phi_i(t;\Psi) \\ N_2[\Phi_i(t;\Psi)] &= \frac{\partial \Phi_i(t;\Psi)}{\partial t} - \theta\Phi_1(t;\Psi) + (\sigma + \eta + \delta_1)\Phi_i(t;\Psi) - \zeta\Phi_4(t;\Psi) \\ N_3[\Phi_i(t;\Psi)] &= \frac{\partial \Phi_i(t;\Psi)}{\partial t} - \sigma\Phi_2(t;\Psi) + (\eta + \delta_2)\Phi_i(t;\Psi) \\ N_4[\Phi_i(t;\Psi)] &= \frac{\partial \Phi_i(t;\Psi)}{\partial t} - \kappa\Phi_1(t;\Psi) + (\zeta + \eta + \phi)\Phi_i(t;\Psi) \\ N_5[\Phi_i(t;\Psi)] &= \frac{\partial \Phi_i(t;\Psi)}{\partial t} - \phi\Phi_4(t;\Psi) + \eta\Phi_i(t;\Psi) \end{aligned} \tag{5}$$

Let $h_i \neq 0$ presumed as an auxiliary parameter and $H_i(t) \neq 0$ presumed as an auxiliary function. By employing the embedded parameter Φ, we reformulate a system of equations as:

$$
\begin{aligned}
(1-\Psi)L[\Phi_1(t;\Psi)-S_0(t)] &= \Psi h_1 H_1(t) N_1[\Phi_1(t;\Psi)] \\
(1-\Psi)L[\Phi_2(t;\Psi)-A_0(t)] &= \Psi h_2 H_2(t) N_2[\Phi_1(t;\Psi)] \\
(1-\Psi)L[\Phi_3(t;\Psi)-T_0(t)] &= \Psi h_3 H_3(t) N_3[\Phi_1(t;\Psi)] \\
(1-\Psi)L[\Phi_4(t;\Psi)-L_0(t)] &= \Psi h_4 H_4(t) N_4[\Phi_1(t;\Psi)] \\
(1-\Psi)L[\Phi_5(t;\Psi)-P_0(t)] &= \Psi h_5 H_5(t) N_5[\Phi_1(t;\Psi)]
\end{aligned} \tag{6}
$$

initial conditions:

$$
\Phi_1(0;\Psi)=S_0,\ \ \Phi_2(0;\Psi)=A_0,\ \ \Phi_3(0;\Psi)=T_0,\ \ \Phi_4(0;\Psi)=L_0,\ \ \Phi_5(0;\Psi)=P_0, \tag{7}
$$

By utilizing the Taylor's theorem and power series expansion in HAM and the m^{th} order deformation in our model, we obtain:

$$
\begin{aligned}
L[S_m(t)-S_{m-1}(t)] &= h_1 H_1(t)[\frac{dS_{m-1}}{dt} - \Omega + (\eta+\theta+\kappa)S_{m-1}] \\
L[A_m(t)-A_{m-1}(t)] &= h_2 H_2(t)[\frac{dA_{m-1}}{dt} - \theta S_{m-1} + (\sigma+\eta+\delta_1)A_{m-1} - \zeta L_{m-1}] \\
L[T_m(t)-T_{m-1}(t)] &= h_3 H_3(t)[\frac{dT_{m-1}}{dt} - \sigma A_{m-1} + (\eta+\delta_2)T_{m-1}] \\
L[L_m(t)-L_{m-1}(t)] &= h_4 H_4(t)[\frac{dL_{m-1}}{dt} - \kappa S_{m-1} + (\zeta+\eta+\phi)L_{m-1}] \\
L[P_m(t)-P_{m-1}(t)] &= h_5 H_5(t)[\frac{dP_{m-1}}{dt} - \phi L_{m-1} + \eta P_{m-1}]
\end{aligned} \tag{8}
$$

By fixing $H_i(t)=1$, the generalized m^{th} order deformation in our model for $m \geq 1$ becomes:

$$
\begin{aligned}
S_m &= \chi_m S_{m-1} + h\int_0^t [\frac{dS_{m-1}}{dt} - \Omega + (\eta+\theta+\kappa)S_{m-1}]dt \\
A_m &= \chi_m A_{m-1} + h\int_0^t [\frac{dA_{m-1}}{dt} - \theta S_{m-1} + (\sigma+\eta+\delta_1)A_{m-1} - \zeta L_{m-1}]dt \\
T_m &= \chi_m T_{m-1} + h\int_0^t [\frac{dT_{m-1}}{dt} - \sigma A_{m-1} + (\eta+\delta_2)T_{m-1}]dt \\
L_m &= \chi_m L_{m-1} + h\int_0^t [\frac{dL_{m-1}}{dt} - \kappa S_{m-1} + (\zeta+\eta+\phi)L_{m-1}]dt \\
P_m &= \chi_m P_{m-1} + h\int_0^t [\frac{dP_{m-1}}{dt} - \phi L_{m-1} + \eta P_{m-1}]dt
\end{aligned} \tag{9}
$$

It is acceptable to use the h-curve as $h_i=-1$ and by substituting the parameter values in Table 1, and Initial values in Table 2, we obtain the following approximations.

Initial approximation:

$$\begin{aligned} S_0 &= 20 \\ A_0 &= 10 \\ T_0 &= 5 \\ L_0 &= 5 \\ P_0 &= 5 \end{aligned} \tag{10}$$

First approximation:

$$\begin{aligned} S_1(t) &= \sum_{m=0}^{1} S_m(t) = 20 - 6.4950t \\ A_1(t) &= \sum_{m=0}^{1} A_m(t) = 10 - 3.0980t \\ T_1(t) &= \sum_{m=0}^{1} T_m(t) = 5 + 5.5710t \\ L_1(t) &= \sum_{m=0}^{1} L_m(t) = 5 + 2.1810t \\ P_1(t) &= \sum_{m=0}^{1} P_m(t) = 5 + 1.4310t \end{aligned} \tag{11}$$

Second approximation:

$$\begin{aligned} S_2(t) &= \sum_{m=0}^{2} S_m(t) = 20 - 6.4950t + 1.155460500t^2 \\ A_2(t) &= \sum_{m=0}^{2} A_m(t) = 10 - 3.0980t + 0.5519012000t^2 \\ T_2(t) &= \sum_{m=0}^{2} T_m(t) = 5 + 5.5710t - 0.9191959000t^2 \\ L_2(t) &= \sum_{m=0}^{2} L_m(t) = 5 + 2.1810t - 1.046223900t^2 \\ P_2(t) &= \sum_{m=0}^{2} P_m(t) = 5 + 1.4310t + 0.3172761000t^2 \end{aligned} \tag{12}$$

Similarly, using the MAPLE program, we calculate the following approximations in infinite series:

(13)

$$S(t) = 20 - 6.4950t + 1.155460500t^2 - 0.1370376153t^3 + 0.01218949588t^4 - 0.0008674045268t^5$$
$$+0.00005143708843t^6 - 2.614473723 \times 10^{-6}t^7 + 1.162787188 \times 10^{-7}t^8 + ...$$
$$A(t) = 10 - 3.0980t + 0.5519012000t^2 - 0.07658408890t^3 + 0.009531508019t^4 - 0.001087406140t^5$$
$$+0.0001110813615t^6 - 9.994153103 \times 10^{-6}t^7 + 7.912145250 \times 10^{-7}t^8 + ...$$
$$T(t) = 5 + 5.5710t - 0.9191959000t^2 + 0.1087824911t^3 - 0.01124719339t^4 + 0.001112601537t^5$$
$$-0.0001053272622t^6 + 9.203591428 \times 10^{-6}t^7 - 7.240141561 \times 10^{-7}t^8 + ...$$
$$L(t) = 5 + 2.1810t - 1.046223900t^2 + 0.2039027849t^3 - 0.02539683904t^4 + 0.002335453844t^5$$
$$-0.0001705198356t^6 + 0.00001033179055t^7 - 5.352000185 \times 10^{-7}t^8 + ...$$
$$P(t) = 5 + 1.4310t + 0.3172761000t^2 - 0.1060818601t^3 + 0.01565869129t^4 - 0.001567028330t^5$$
$$+0.0001203768574t^6 - 7.545307329 \times 10^{-6}t^7 + 4.004578008 \times 10^{-7}t^8 + ...$$

3.2. Homotopy Perturbation Method. In this subsection, we apply Homotopy perturbation method for the T2D model. First we constract the Homotopy for (1).

(14)
$$\begin{aligned}
(1-p)\frac{dS}{dt} + p[\frac{dS}{dt} - \Omega + (\eta + \theta + \kappa)S = 0] \\
(1-p)\frac{dA}{dt} + p[\frac{dA}{dt} - \theta S + (\sigma + \eta + \delta_1)A - \zeta L = 0] \\
(1-p)\frac{dT}{dt} + p[\frac{dT}{dt} - \sigma A + (\eta + \delta_2)T = 0] \\
(1-p)\frac{dL}{dt} + p[\frac{dL}{dt} - \kappa S + (\zeta + \eta + \phi)L = 0] \\
(1-p)\frac{dP}{dt} + p[\frac{dP}{dt} - \phi L + \eta P = 0]
\end{aligned}$$

Essentially, the solution to Equation (1) is presumed to be a series in powers of p.

$$S(t) = S_0 + pS_1 + p^2S_2 + ...$$
$$A(t) = A_0 + pA_1 + p^2A_2 + ...$$
$$T(t) = T_0 + pT_1 + p^2T_2 + ...$$
$$L(t) = L_0 + pL_1 + p^2L_2 + ...$$

$$P(t) = P_0 + pP_1 + p^2P_2 + ...$$

Examine the equivalent powers of p, we obtain:

$$\begin{aligned} p^0 &: S_0^{'} = 0 \\ p^1 &: S_1^{'} - \Omega + (\eta + \theta + \kappa)S_0 = 0 \\ p^2 &: S_2^{'} + (\eta + \theta + \kappa)S_1 = 0 \end{aligned} \tag{15}$$

$$\begin{aligned} p^0 &: A_0^{'} = 0 \\ p^1 &: A_1^{'} - \theta S_0 + (\sigma + \eta + \delta_1)A_0 - \zeta L_0 = 0 \\ p^2 &: A_2^{'} - \theta S_1 + (\sigma + \eta + \delta_1)A_1 - \zeta L_1 = 0 \end{aligned} \tag{16}$$

$$\begin{aligned} p^0 &: T_0^{'} = 0 \\ p^1 &: T_1^{'} - \sigma A_0 + (\eta + \delta_2)T_0 = 0 \\ p^2 &: T_2^{'} - \sigma A_1 + (\eta + \delta_2)T_1 = 0 \end{aligned} \tag{17}$$

$$\begin{aligned} p^0 &: L_0^{'} = 0 \\ p^1 &: L_1^{'} - \kappa S_0 + (\zeta + \eta + \phi)L_0 = 0 \\ p^2 &: L_2^{'} - \kappa S_1 + (\zeta + \eta + \phi)L_1 = 0 \end{aligned} \tag{18}$$

$$\begin{aligned} p^0 &: P_0^{'} = 0 \\ p^1 &: P_1^{'} - \phi L_0 + \eta P_0 = 0 \\ p^2 &: P_2^{'} - \phi L_1 + \eta P_1 = 0 \end{aligned} \tag{19}$$

Solving (15)-(19) by direct integration method for p^0 using Table 1 and Table 2 values, we obtain:

$$S_0 = 20$$

$$A_0 = 10$$

$$T_0 = 5$$
$$L_0 = 5 \tag{20}$$
$$P_0 = 5$$

Substituting (20) into (15)-(19) and solve by direct integration method for p^1, we obtain:

$$S_1 = 6.4950t$$
$$A_1 = 3.0980t$$
$$T_1 = 5.5710t \tag{21}$$
$$L_1 = 2.1810t$$
$$P_1 = 1.4310t$$

Substituting (21) into (15)-(19) and solve by direct integration method for p^2, we obtain:

$$S_2 = 1.155460500t^2$$
$$A_2 = 0.5519012000t^2$$
$$T_2 = -0.9191959000t^2 \tag{22}$$
$$L_2 = -1.046223900t^2$$
$$P_2 = 0.3172761000t^2$$

Similarly, we make use of the MAPLE software to compute the approximations in infinite series:

$$S(t) = 20 - 6.4950t + 1.155460500t^2 - 0.1370376153t^3 + 0.01218949588t^4 - 0.0008674045268t^5$$
$$+0.00005143708843t^6 - 2.614473723 \times 10^{-6}t^7 + 1.162787188 \times 10^{-7}t^8 + ...$$
$$A(t) = 10 - 3.0980t + 0.5519012000t^2 - 0.07658408890t^3 + 0.009531508019t^4 - 0.001087406140t^5$$
$$+0.0001110813615t^6 - 9.994153103 \times 10^{-6}t^7 + 7.912145250 \times 10^{-7}t^8 + ...$$
$$T(t) = 5 + 5.5710t - 0.9191959000t^2 + 0.1087824911t^3 - 0.01124719339t^4 + 0.001112601537t^5$$
$$-0.0001053272622t^6 + 9.203591428 \times 10^{-6}t^7 - 7.240141561 \times 10^{-7}t^8 + ...$$

(23)

$$L(t) = 5 + 2.1810t - 1.046223900t^2 + 0.2039027849t^3 - 0.02539683904t^4 + 0.002335453844t^5$$
$$-0.0001705198356t^6 + 0.00001033179055t^7 - 5.352000185 \times 10^{-7}t^8 + ...$$
$$P(t) = 5 + 1.4310t + 0.3172761000t^2 - 0.1060818601t^3 + 0.01565869129t^4 - 0.001567028330t^5$$
$$+0.0001203768574t^6 - 7.545307329 \times 10^{-6}t^7 + 4.004578008 \times 10^{-7}t^8 + ...$$

4. Discussion of Results

The concentration profiles S, A, T, L, and P in T2D were determined by solving the system of equations using HAM and HPM. The analytical solutions for T2D are represented by Equations (13) and (23). Notably, when setting $h = -1$ in HAM, it is evident that both the HAM and HPM solutions are same. Utilizing the Runge-Kutta method, a numerical implementation of a system of equations (1) is developed. The numerical simulations were performed using MATLAB. In this analysis, we assume the initial populations of 20 individuals in the Susceptible class, 10 individuals in the Affected class, 5 individuals in the Treated class, 5 individuals in the Healthy Lifestyle class, and 5 individuals in the Prevented class, thereby establishing the system's initial conditions as $S(0) = 20$, $A(0) = 10$, $T(0) = 5$, $L(0) = 5$, $P(0) = 5$, as outlined in Table 2. The parameter values listed in Table 1 were used in the analysis. Figures 2.a-2.e depicts graphical representations illustrating the efficiency of the HPM and HAM solutions for the concentrations S, A, T, L, and P, along with the corresponding numerical results considering the parameter values in Table 1. Tables 3, 4, 5, 6, and 7 show the accuracy of our analytical expressions for concentrations S, A, T, L, and R. The comparison reveals that the overall error between the HAM and HPM with the numerical simulation remains below 0.1% and 0.1%, respectively. From the figures and tables, it is clear that both methods consistently offer a more accurate approximation even within a limited time interval.

4.1. Behaviour of the parameters in T2D. As the parameters Ω and η increased, Figures 3.a-3. b indicates a corresponding increase in the susceptible class. Conversely, an increase in parameters θ and κ is associated with a decrease in the susceptible class, as shown in Figures 3.c-3.d. Figure 13 shows the surface plots of $S(t)$ with respect to (a) Ω and time, (b) η and time, (c) θ and time, and (d) κ and time. Similarly, Figures 4.a-4.b shows that an increase in parameters θ and ζ leads to an increase in the affected class. On the other hand, an increase in the parameters σ, η, and δ_1 results in a decrease in the affected class, as depicted in Figures 4.c-4.e. Figure 14 presents surface plots for $A(t)$ with respect to (a) θ and time, (b) ζ and time, (c) σ and time, (d) η and time, and (e) δ_1 and time. Furthermore, an increase in the parameters σ and η corresponds to an increase in the treated class, as shown in Figures 5.a-5.b, while an increase in the parameter δ_2 leads to a decrease in the treated class, as observed in Figure 5.c. Figure 15 shows the surface plots of $T(t)$ with respect to (a) σ and time, (b) η and time, and (c) δ_2 and time. Additionally, an increase in the parameter κ is associated with an increase in the healthy lifestyle class, as indicated in Figure 6.a. However, an increase in the parameters ζ, η, and ϕ leads to a decrease in the healthy lifestyle class, as shown in Figures 6.b-6.d. Figure 16 illustrates surface plots for $L(t)$ with respect to (a) κ and time, (b) ζ and time, (c) η and time, and (d) ϕ and time. Finally, an increase in parameter ϕ results in an increase in the prevented class, as shown in Figure 7.a, whereas an increase in the parameter η corresponds to a decrease in the prevented class, as depicted in Figure 7.b. Figure 17 presents surface plots for $P(t)$ with respect to (a) ϕ and time, and (b) η and time.

4.2. h-curve. The convergence and accuracy of the resulting series are controlled by the auxiliary parameter h. Multiple h-curves are displayed to designate a region such that the resulting series is independent of h. The complete convergence region was defined as the common region between and its derivatives. To observe how h influences the convergence of the solution, h-curves are produced for each concentration S, A, T, L, and P. Figure 8 shows the h-curve of $3rd$ and $4th$ order approximate solutions of $S(t)$ and $S'(t)$ at $t = 0.3$, where the horizontal line denotes the convergence region. Similarly, Figure 9 shows the corresponding h-curve of $A(t)$ at $t = 0.6$. Figure 10 shows the corresponding h-curve of $T(t)$ at $t = 0.6$. Figure 11 shows the corresponding h-curve of $L(t)$ at $t = 0.2$, and Figure 12 shows the corresponding h-curve of $P(t)$

at $t = 0.65$. For the corresponding function, the convergence region is the horizontal line that represents the region where the concentrations S, A, T, L, and P versus h are found and clearly shows that the range of h that is valid is approximately $(-1.1$ to $-0.7)$ in our T2D model, as shown in Table 8.

5. CONCLUSION

This study examined an ordinary differential equation describing an epidemiological model of type 2 diabetes. We used both the Homotopy Analysis Method (HAM) and Homotopy Perturbation Method (HPM) to obtain semi-analytical solutions for the type 2 diabetes SATLP model. Epidemiological problems are frequently solved using both the approaches. When homotopy h is set to -1, both HAM and HPM yield identical outcomes. This is due to the fact that at $h = -1$, the original equation in the homotopy formulation equals the target linear and nonlinear equation, leading to convergence. A comparison was made between the analytical and numerical simulation findings, and good agreement was obtained. Using the h-curves, the convergence region in the HAM was established. To determine the behavior of the model, parameter values were computed using both semi-analytical methods and numerical simulations. Furthermore, we observed that the increase in diabetes rate from susceptibility over time led to an increase in the affected population and an increase in the treatment rate over time, leading to a decrease in the affected population and an increase in the recovered population. A healthy lifestyle can help delay or avoid the development of T2D, slow disease progression, and reduce the effects of the disease by using appropriate control strategies and therapies.

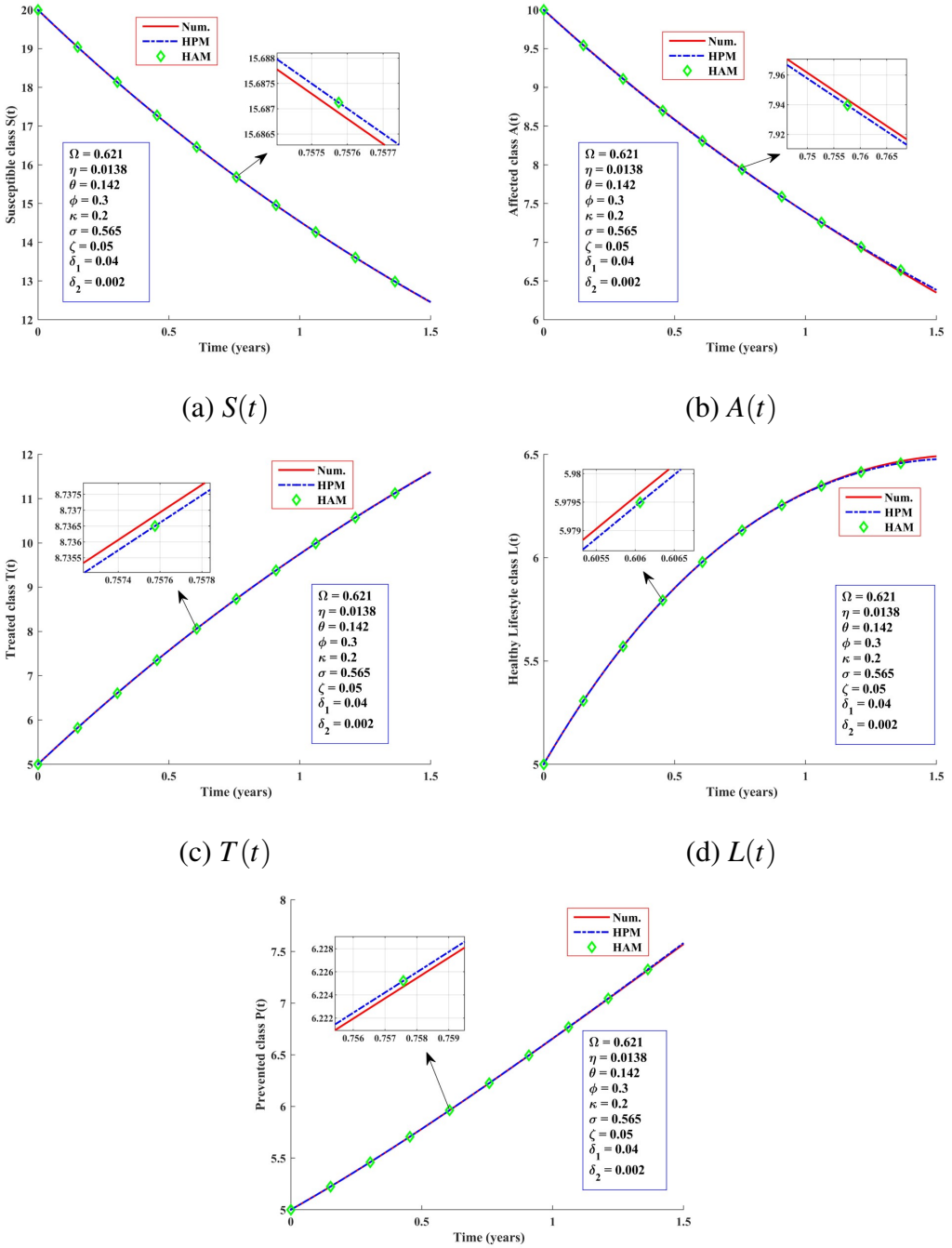

(a) $S(t)$ (b) $A(t)$

(c) $T(t)$ (d) $L(t)$

(e) $P(t)$

FIGURE 2. Graphical representation of analytical expressions obtained by HPM and HAM with numerical simulation for the parameter values provided in Table 1 and initial values in Table 2.

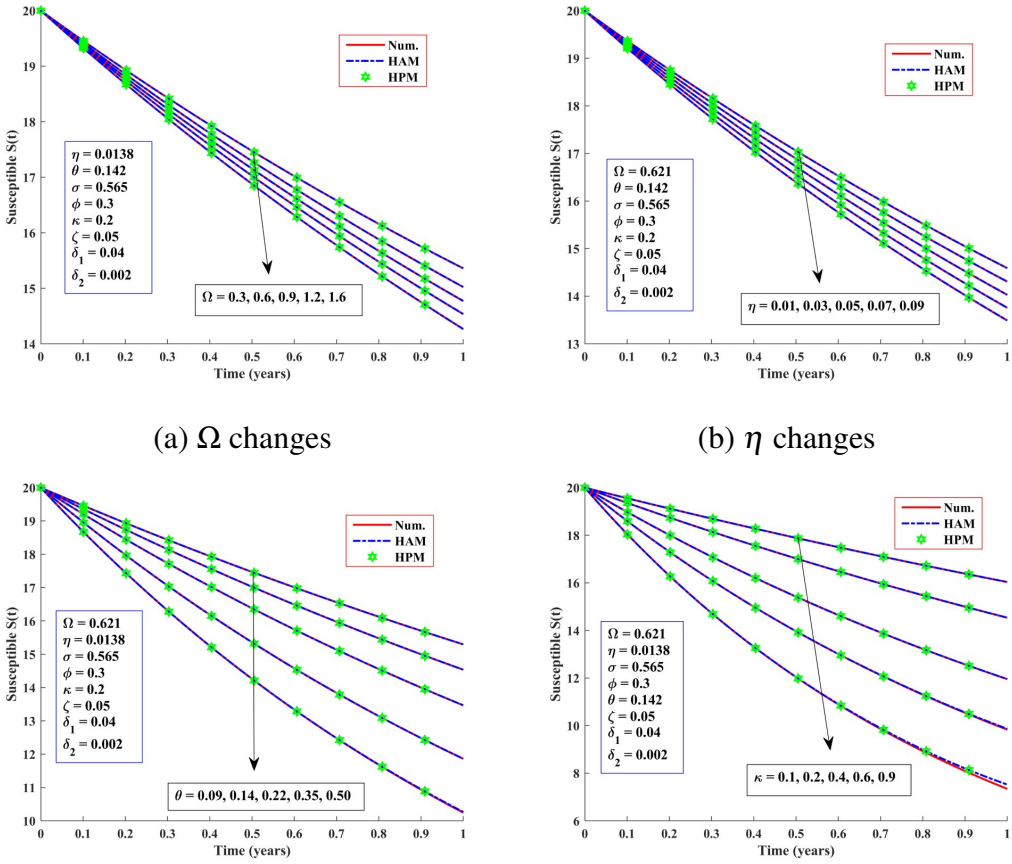

(a) Ω changes

(b) η changes

(c) θ changes

(d) κ changes

FIGURE 3. Behavior of parameters in $S(t)$ when (a) $\Omega = 0.3, 0.6, 0.9, 1.2, 1.5$, (b) $\eta = 0.01, 0.03, 0.05, 0.07, 0.09$, (c) $\theta = 0.09, 0.14, 0.22, 0.35, 0.50$, (d) $\kappa = 0.1, 0.2, 0.4, 0.6, 0.9$.

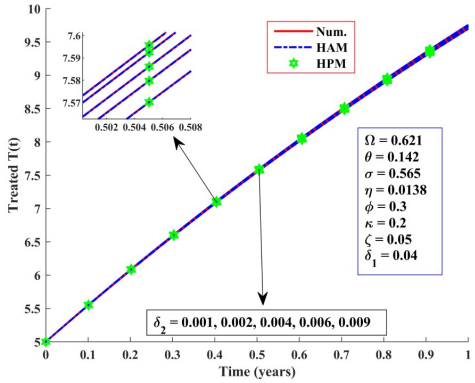

(a) δ_2 changes

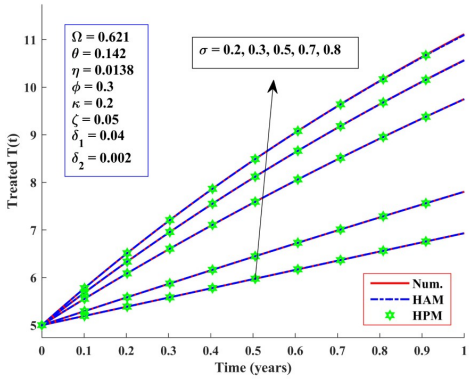

(b) σ changes

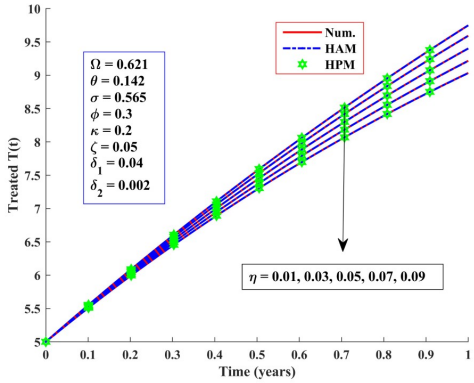

(c) η changes

FIGURE 5. Behavior of parameters in $T(t)$ when

(a) $\delta_2 = 0.01, 0.03, 0.05, 0.07, 0.09$, (b) $\sigma = 0.2, 0.3, 0.5, 0.7, 0.8$,

(c) $\eta = 0.01, 0.03, 0.05, 0.07, 0.09$.

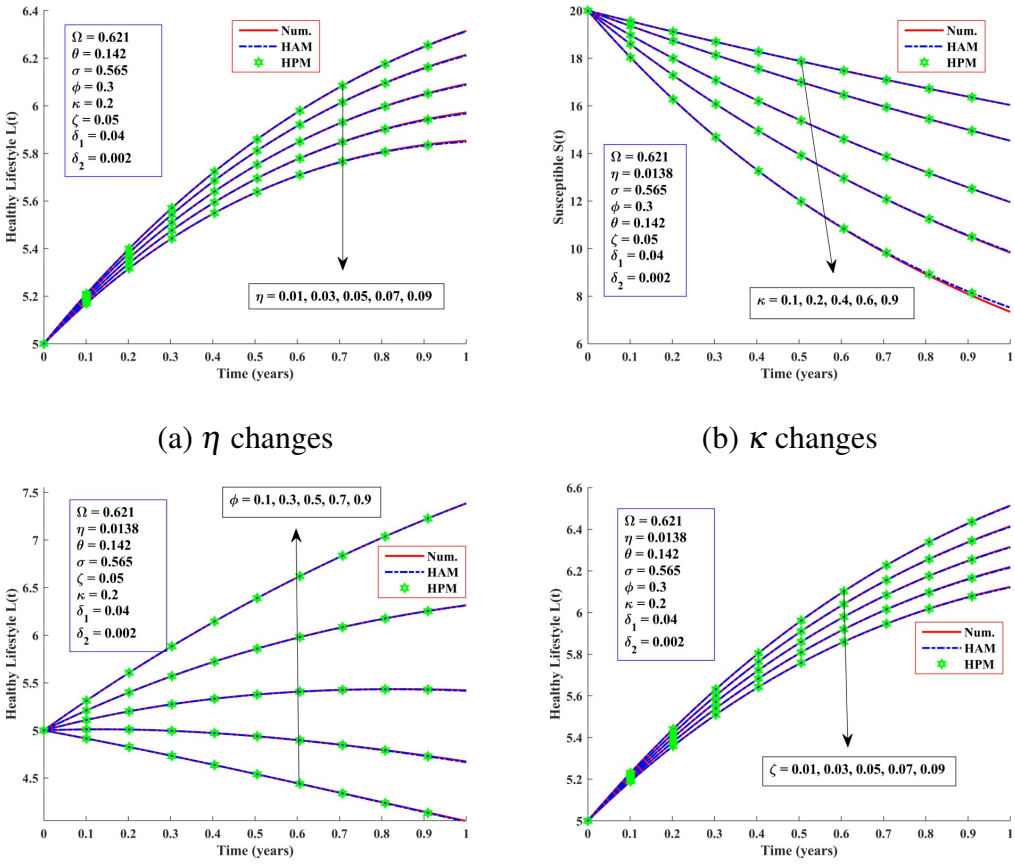

(a) η changes (b) κ changes

(c) ϕ changes (d) ζ changes

FIGURE 6. Behavior of parameters in $L(t)$ when

(a) $\eta = 0.01, 0.03, 0.05, 0.07, 0.09$, (b) $\kappa = 0.1, 0.2, 0.4, 0.6, 0.9$,

(c) $\phi = 0.1, 0.3, 0.5, 0.7, 0.9$, (d) $\zeta = 0.01, 0.03, 0.05, 0.07, 0.09$.

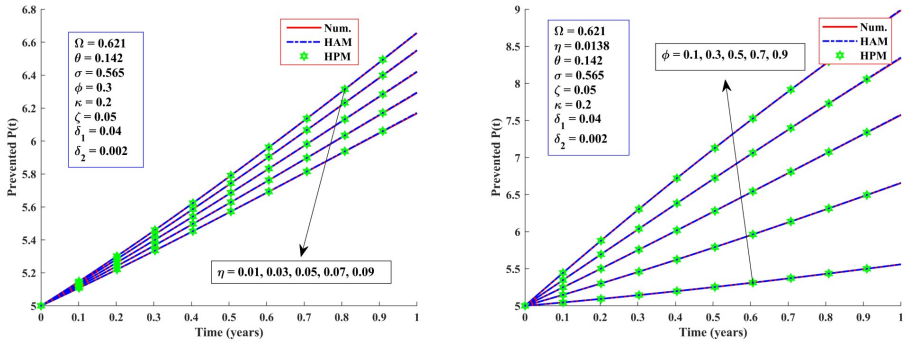

(a) η changes (b) ϕ changes

FIGURE 7. Behavior of parameters in $P(t)$ when
(a) $\eta = 0.01, 0.03, 0.05, 0.07, 0.09$, (b) $\phi = 0.1, 0.3, 0.5, 0.7, 0.9$.

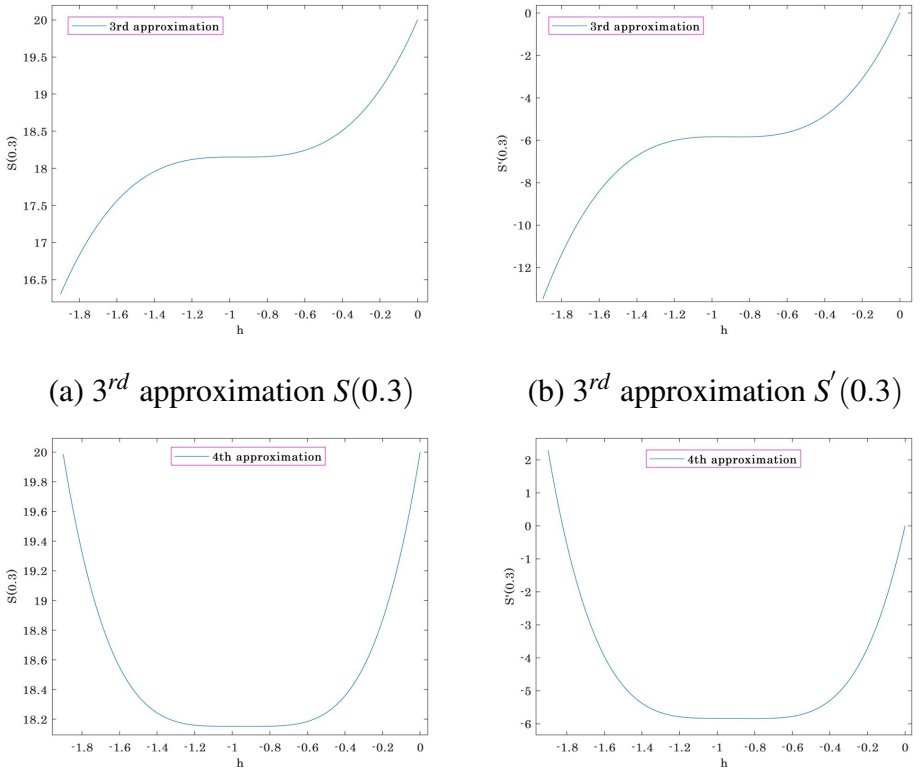

(a) 3^{rd} approximation $S(0.3)$ (b) 3^{rd} approximation $S'(0.3)$

(c) 4^{th} approximation $S(0.3)$ (d) 4^{th} approximation $S'(0.3)$

FIGURE 8. h-curves in $S(t)$.

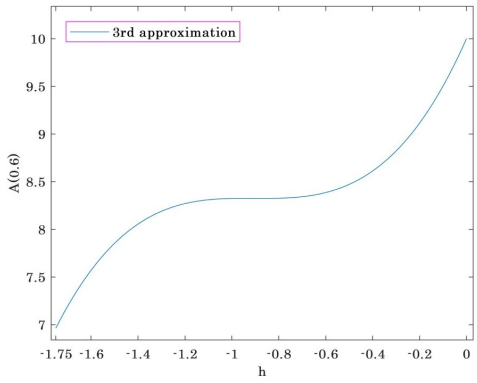

(a) 3^{rd} approximation $A(0.6)$

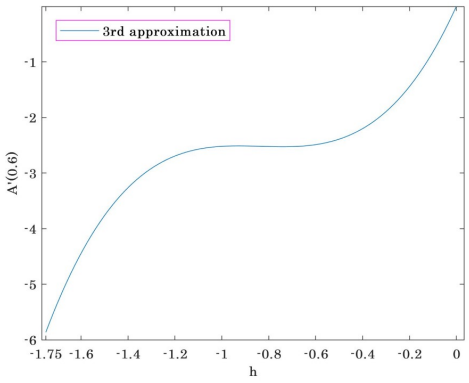

(b) 3^{rd} approximation $A^{'}(0.6)$

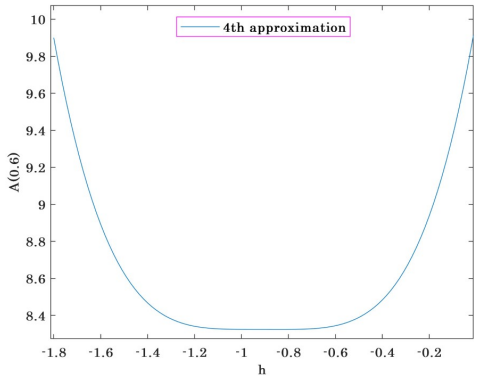

(c) 4^{th} approximation $A(0.6)$

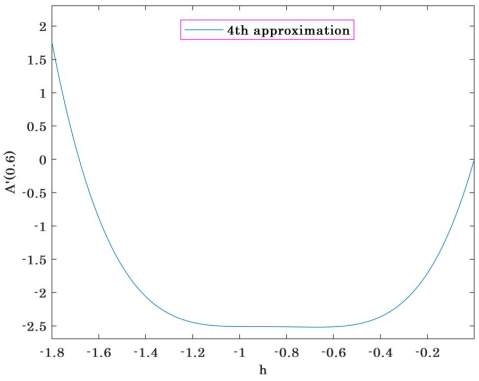

(d) 4^{th} approximation $A^{'}(0.6)$

FIGURE 9. h-curves in $A(t)$.

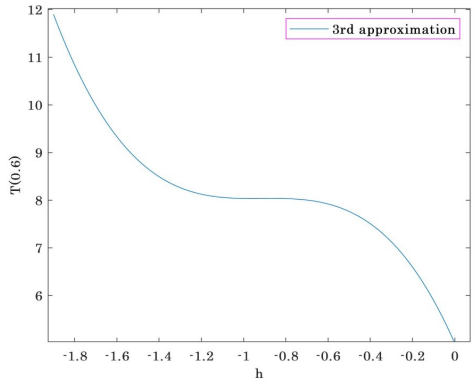

(a) 3^{rd} approximation $T(0.6)$

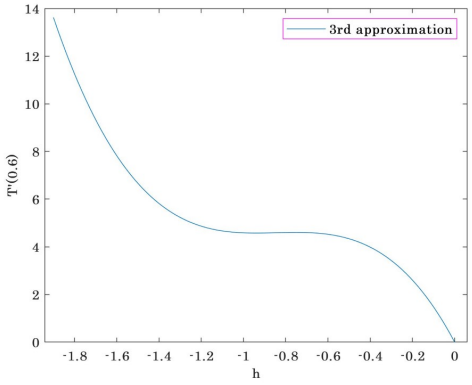

(b) 3^{rd} approximation $T^{'}(0.6)$

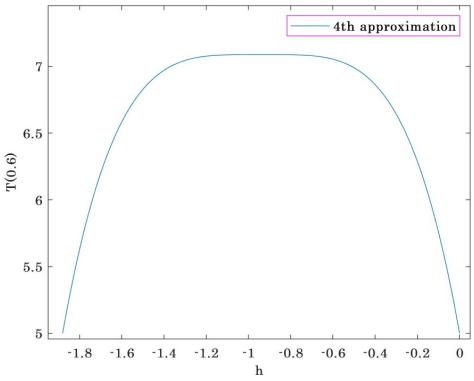

(c) 4^{th} approximation $T(0.6)$

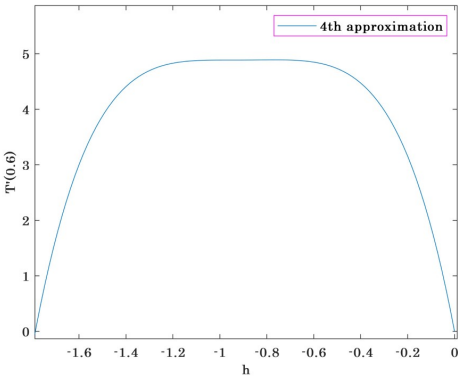

(d) 4^{th} approximation $T^{'}(0.6)$

FIGURE 10. h-curves in $T(t)$.

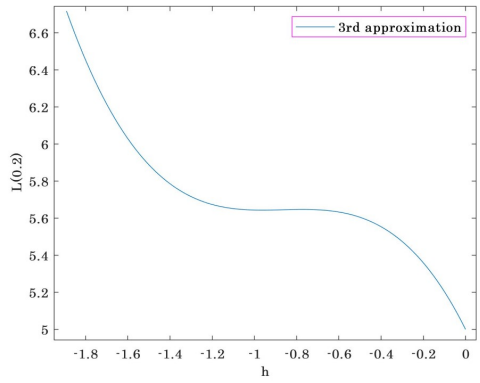

(a) 3^{rd} approximation $L(0.35)$

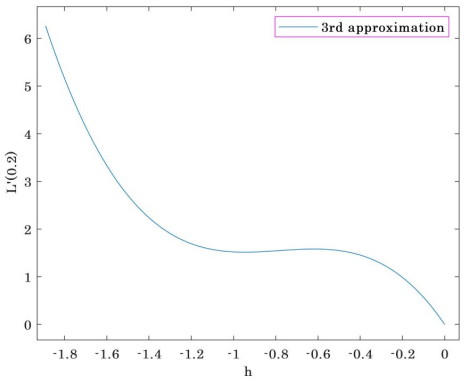

(b) 3^{rd} approximation $L^{'}(0.35)$

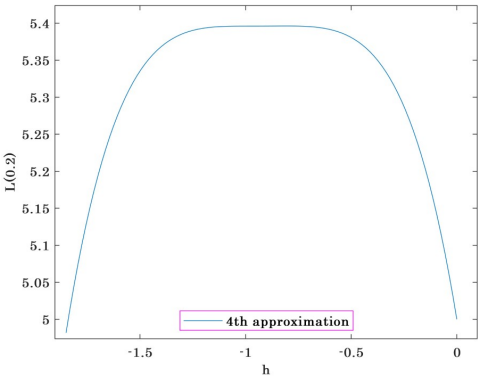

(c) 4^{th} approximation $L(0.35)$

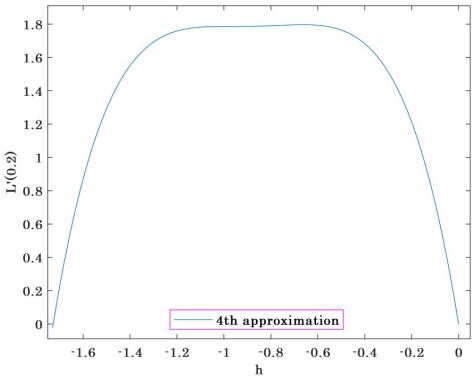

(d) 4^{th} approximation $L^{'}(0.35)$

FIGURE 11. h-curves in $L(t)$.

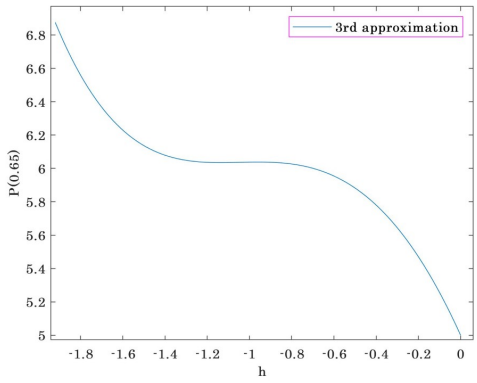

(a) 3^{rd} approximation $P(0.65)$

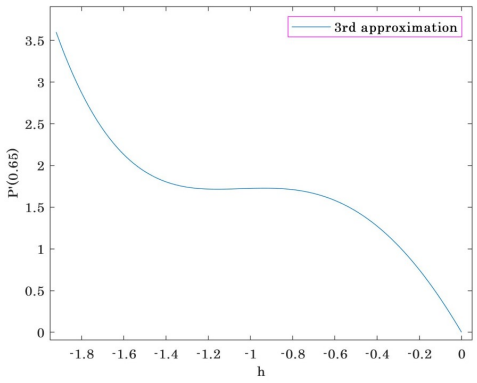

(b) 3^{rd} approximation $P^{'}(0.65)$

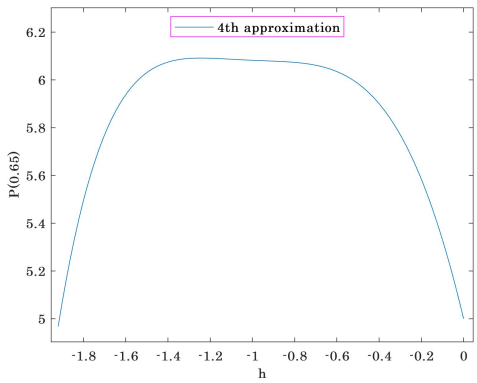

(c) 4^{th} approximation $P(0.65)$

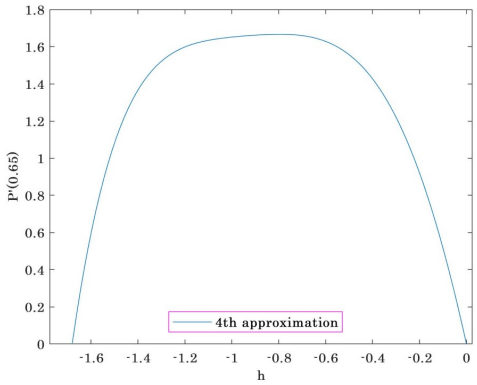

(d) 4^{th} approximation $P^{'}(0.65)$

FIGURE 12. h-curves in $P(t)$.

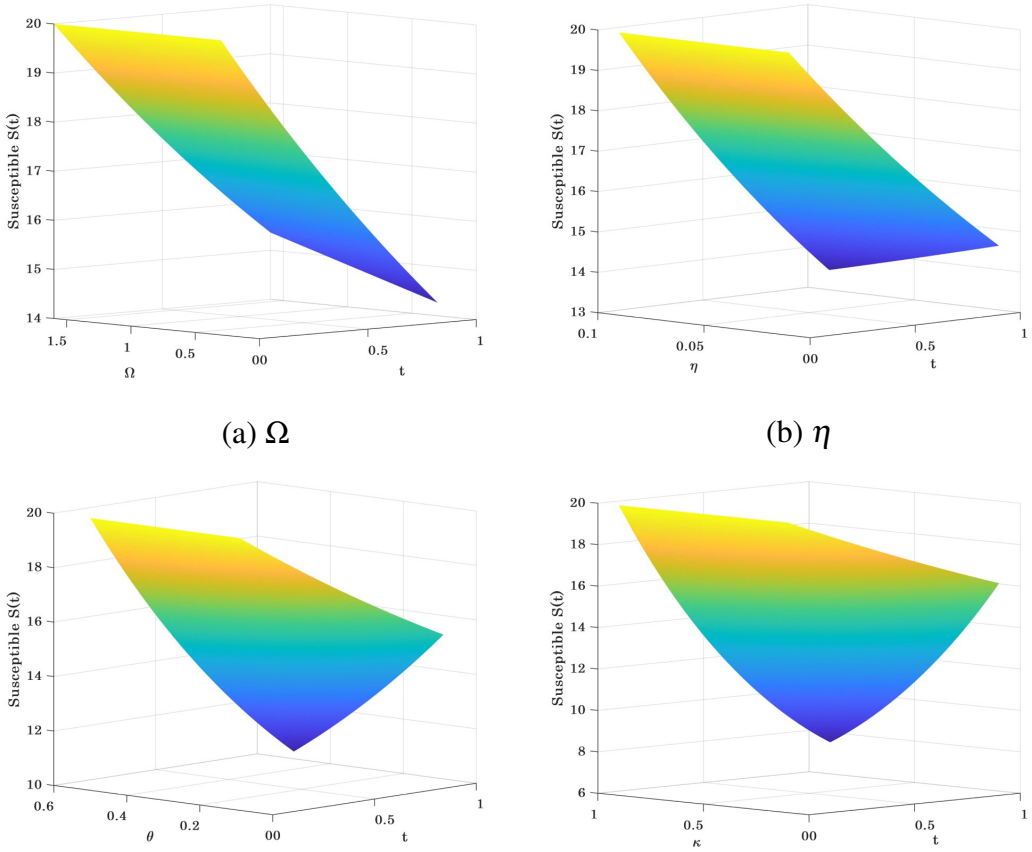

(a) Ω (b) η

(c) θ (d) κ

FIGURE 13. Susceptible T2D model using different values of the parameters Ω, η, θ, and κ.

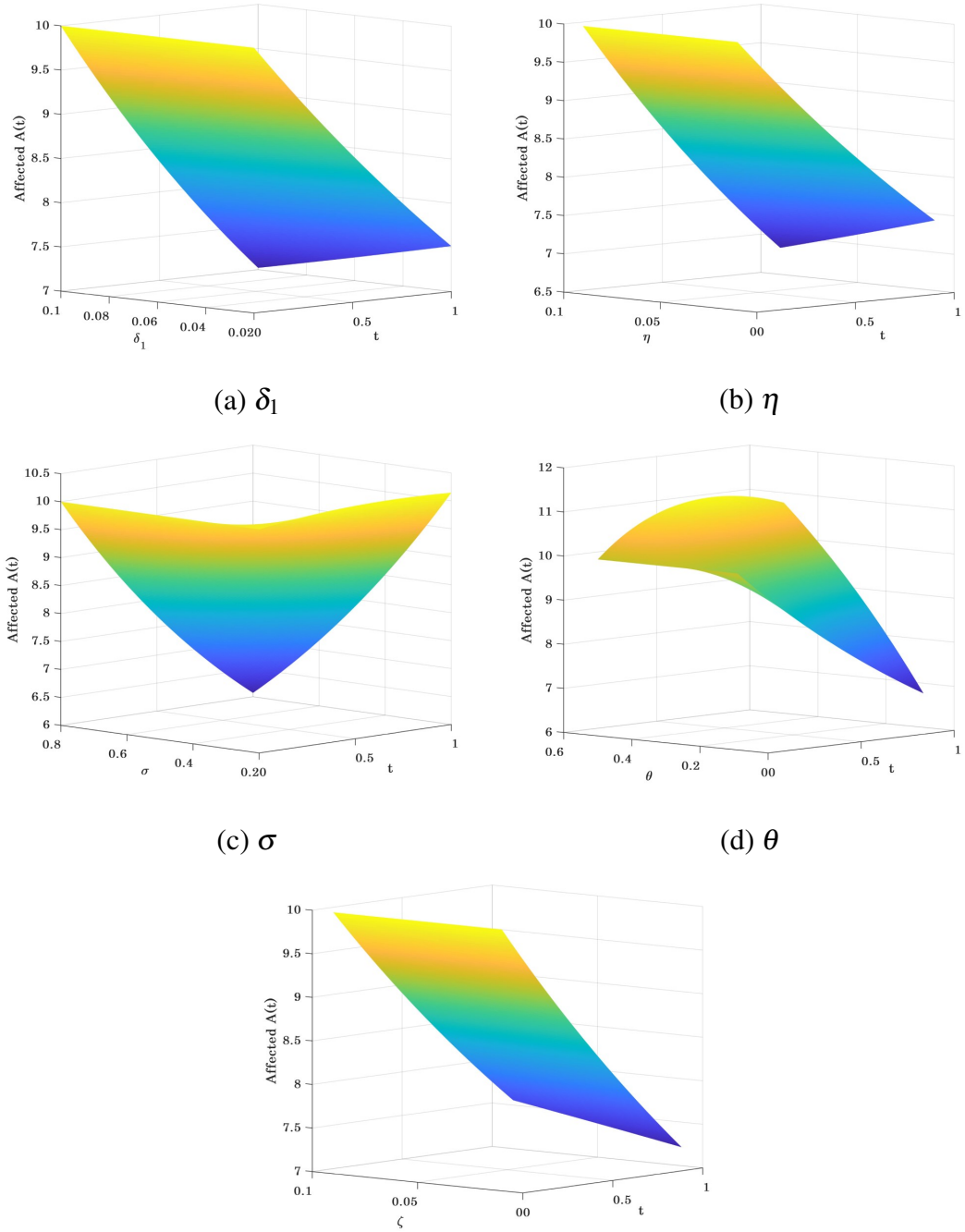

FIGURE 14. Affected T2D model using different values of the parameters δ_1, η, σ, θ, and ζ.

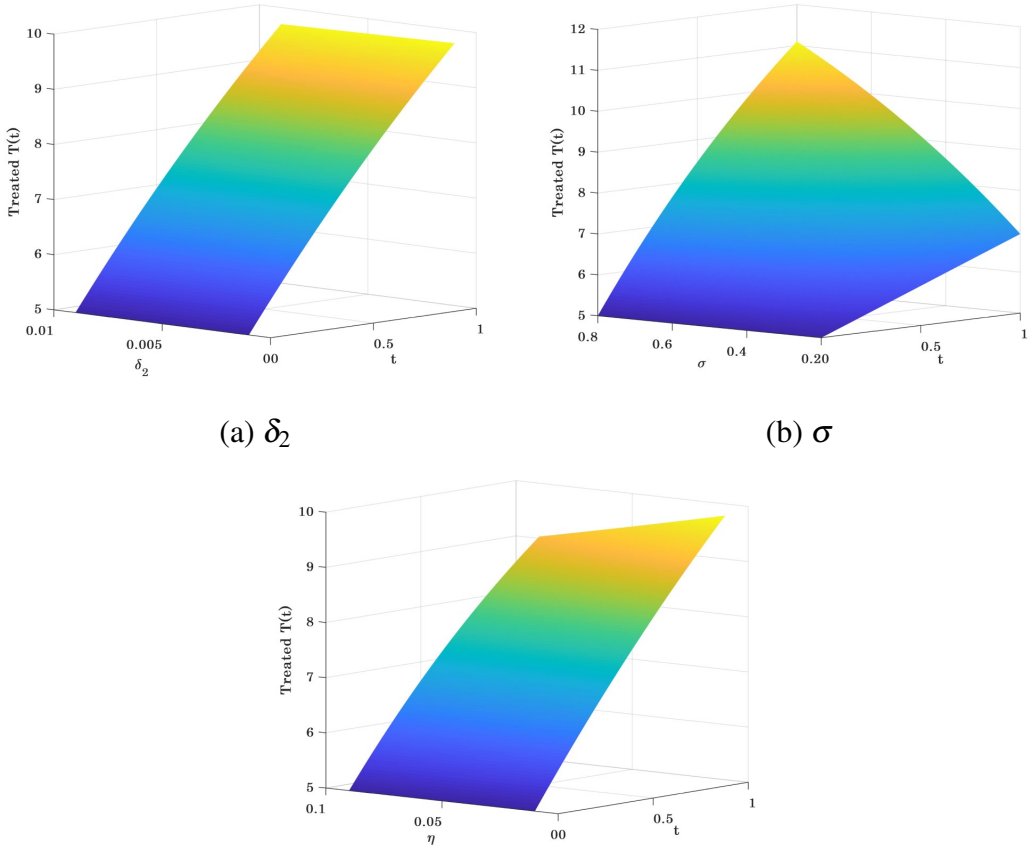

(a) δ_2 (b) σ

(c) η

FIGURE 15. Treated T2D model using different values of the parameters δ_2, η, and σ.

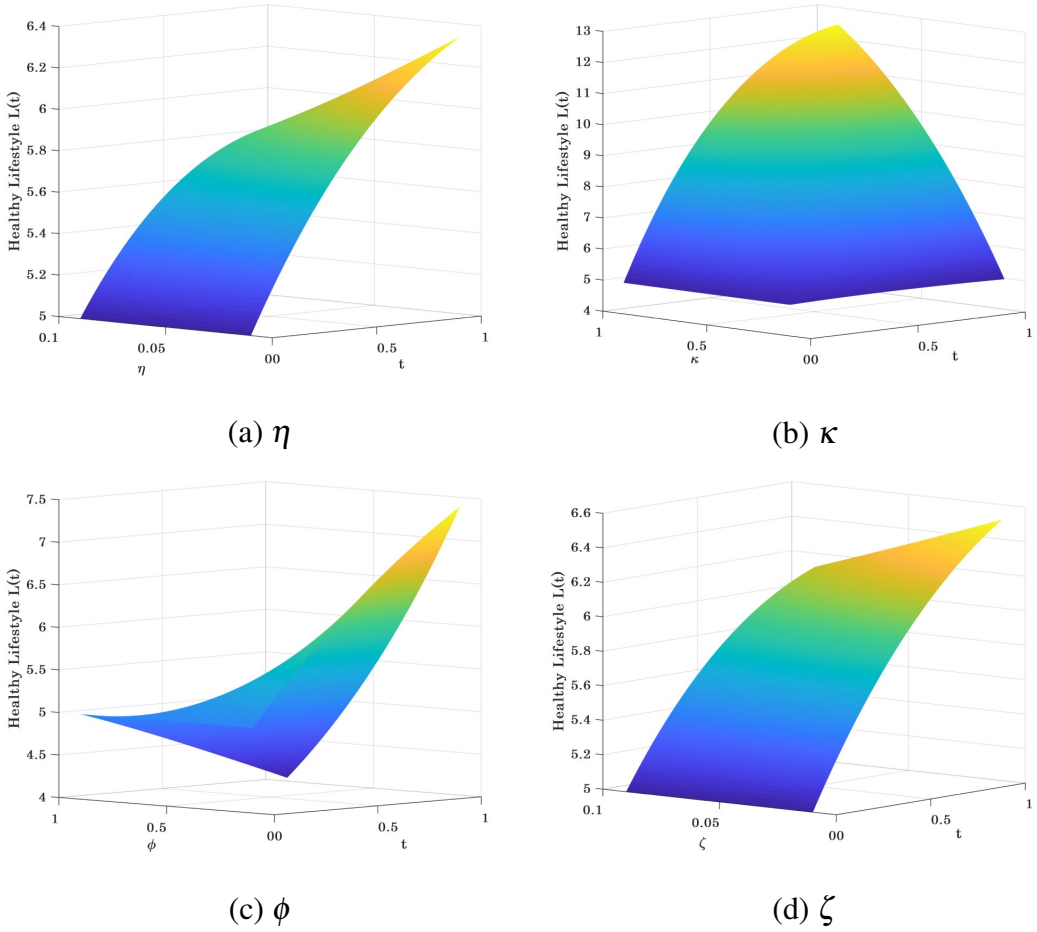

(a) η (b) κ

(c) ϕ (d) ζ

FIGURE 16. Healthy Lifestyle T2D model using different values of the parameters κ, η, ϕ, and ζ.

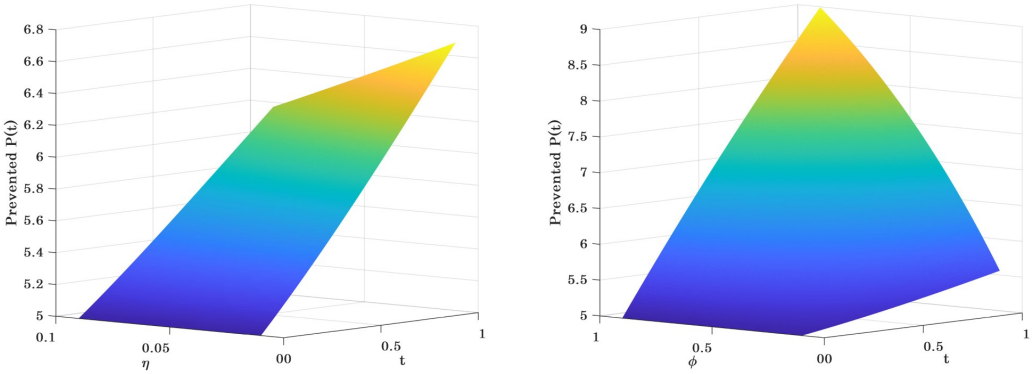

(a) η (b) ϕ

FIGURE 17. Prevented T2D model using different values of the parameters η and ϕ.

TABLE 3. Comparison of HAM and HPM with numerical results for the concentration profile S

Susceptible class S(t)					
t	Num.	HAM	HPM	HAM Error%	HPM Error%
0	20.0000	20.0000	20.0000	0.0000	0.0000
0.1	19.3619	19.3619	19.3619	0.0000	0.0000
0.2	18.7461	18.7461	18.7461	0.0000	0.0000
0.3	18.1519	18.1519	18.1519	0.0000	0.0000
0.4	17.5784	17.5784	17.5784	0.0000	0.0000
0.5	17.0250	17.0250	17.0250	0.0000	0.0000
0.6	16.4909	16.4909	16.4909	0.0000	0.0000
0.7	15.9755	15.9756	15.9756	0.0006	0.0006
0.8	15.4781	15.4783	15.4783	0.0013	0.0013
0.9	14.9980	14.9985	14.9985	0.0033	0.0033
1	14.5348	14.5356	14.5356	0.0055	0.0055
Average error %				0.0009	0.0009

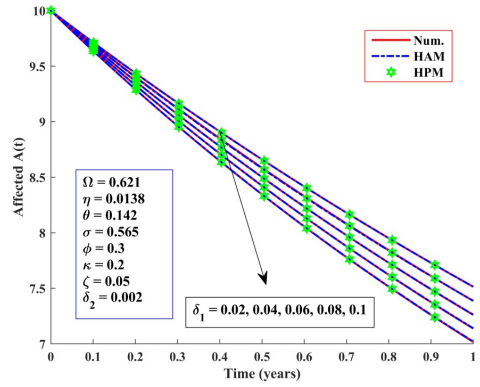

(a) δ_1 changes

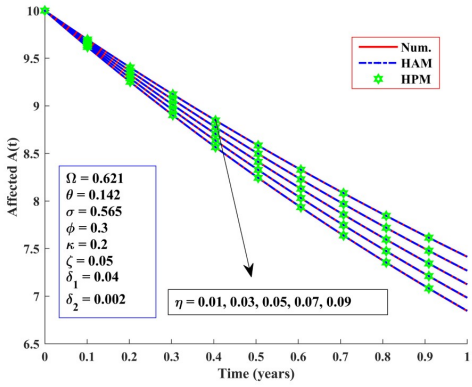

(b) η changes

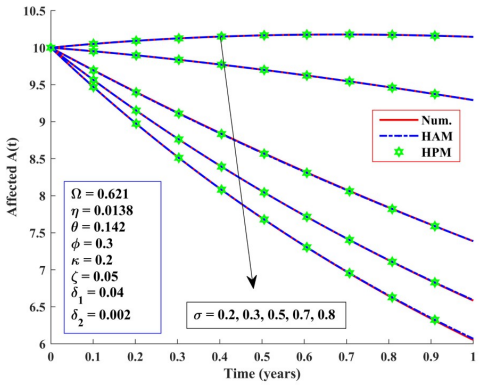

(c) σ changes

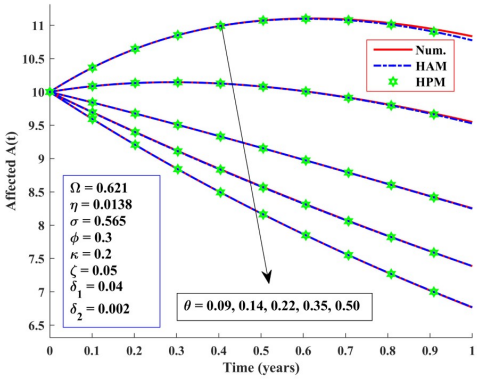

(d) θ changes

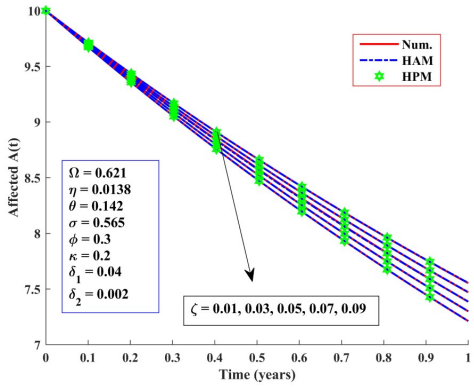

(e) ζ changes

FIGURE 4. Behavior of parameters in $A(t)$ when

(a) $\delta_1 = 0.02, 0.04, 0.06, 0.08, 0.1$, (b) $\eta = 0.01, 0.03, 0.05, 0.07, 0.09$,

(c) $\sigma = 0.2, 0.3, 0.5, 0.7, 0.8$, (d) $\theta = 0.09, 0.14, 0.22, 0.35, 0.50$,

(e) $\zeta = 0.01, 0.03, 0.05, 0.07, 0.09$.

TABLE 4. Comparison of HAM and HPM with numerical results for the concentration profile A

Affected class A(t)					
t	Num.	HAM	HPM	HAM Error%	HPM Error%
0	10.0000	10.0000	10.0000	0.0000	0.0000
0.1	9.6985	9.6956	9.6956	0.0299	0.0299
0.2	9.4056	9.4019	9.4019	0.0393	0.0393
0.3	9.1227	9.1183	9.1183	0.0482	0.0482
0.4	8.8492	8.8444	8.8444	0.0542	0.0542
0.5	8.5849	8.5800	8.5800	0.0571	0.0571
0.6	8.3294	8.3246	8.3246	0.0576	0.0576
0.7	8.0821	8.0779	8.0779	0.0520	0.0520
0.8	7.8427	7.8395	7.8395	0.0408	0.0408
0.9	7.6108	7.6093	7.6093	0.0197	0.0197
1	7.3858	7.3868	7.3868	0.0135	0.0135
Average error %				0.0374	0.0374

TABLE 5. Comparison of HAM and HPM with numerical results for the concentration profile T

Treated class T(t)					
t	Num.	HAM	HPM	HAM Error%	HPM Error%
0	5.0000	5.0000	5.0000	0.0000	0.0000
0.1	5.5480	5.5480	5.5480	0.0000	0.0000
0.2	6.0783	6.0783	6.0783	0.0000	0.0000
0.3	6.5914	6.5914	6.5914	0.0000	0.0000
0.4	7.0880	7.0880	7.0880	0.0000	0.0000
0.5	7.5687	7.5686	7.5686	0.0013	0.0013
0.6	8.0339	8.0337	8.0337	0.0025	0.0025
0.7	8.4841	8.4839	8.4839	0.0024	0.0024
0.8	8.9200	8.9196	8.9196	0.0045	0.0045
0.9	9.3420	9.3413	9.3413	0.0075	0.0075
1	9.7504	9.7493	9.7493	0.0113	0.0113
Average error %				0.0026	0.0026

TABLE 6. Comparison of HAM and HPM with numerical results for the concentration profile L

Healthy Lifestyle class L(t)					
t	Num.	HAM	HPM	HAM Error%	HPM Error%
0	5.0000	5.0000	5.0000	0.0000	0.0000
0.1	5.2078	5.2078	5.2078	0.0000	0.0000
0.2	5.3960	5.3959	5.3959	0.0019	0.0019
0.3	5.5655	5.5654	5.5654	0.0018	0.0018
0.4	5.7175	5.7174	5.7174	0.0017	0.0017
0.5	5.8529	5.8528	5.8528	0.0017	0.0017
0.6	5.9729	5.9727	5.9727	0.0033	0.0033
0.7	6.0782	6.0779	6.0779	0.0049	0.0049
0.8	6.1699	6.1692	6.1692	0.0113	0.0113
0.9	6.2486	6.2474	6.2474	0.0192	0.0192
1	6.3153	6.3133	6.3133	0.0317	0.0317
Average error %				0.0071	0.0071

TABLE 7. Comparison of HAM and HPM with numerical results for the concentration profile P

Prevented class P(t)					
t	Num.	HAM	HPM	HAM Error%	HPM Error%
0	5.0000	5.0000	5.0000	0.0000	0.0000
0.1	5.1462	5.1462	5.1462	0.0000	0.0000
0.2	5.2980	5.2981	5.2981	0.0019	0.0019
0.3	5.4551	5.4551	5.4551	0.0000	0.0000
0.4	5.6167	5.6168	5.6168	0.0018	0.0018
0.5	5.7824	5.7825	5.7825	0.0017	0.0017
0.6	5.9517	5.9519	5.9519	0.0034	0.0034
0.7	6.1242	6.1245	6.1245	0.0049	0.0049
0.8	6.2993	6.3000	6.3000	0.0111	0.0111
0.9	6.4768	6.4778	6.4778	0.0154	0.0154
1	6.6562	6.6579	6.6579	0.0255	0.0255
Average error %				0.0059	0.0059

TABLE 8. The accepted range of h obtained from Figures 8 to 12

Variables	h-curve range
$S(t)$	$-1.2 \leq h \leq -0.7$
$A(t)$	$-1.1 \leq h \leq -0.6$
$T(t)$	$-1.2 \leq h \leq -0.6$
$L(t)$	$-1.1 \leq h \leq -0.6$
$P(t)$	$-1.3 \leq h \leq -0.7$

CONFLICT OF INTERESTS

The authors declare that there is no conflict of interests.

REFERENCES

[1] R.A. DeFronzo, E. Ferrannini, L. Groop, et al. Type 2 diabetes mellitus, Nat. Rev. Dis. Primers 1 (2015), 15019. https://doi.org/10.1038/nrdp.2015.19.

[2] P. Aschner, S. Karuranga, S. James, et al. The international diabetes federation's guide for diabetes epidemiological studies, Diabetes Res. Clin. Pract. 172 (2021), 108630. https://doi.org/10.1016/j.diabres.2020.108630.

[3] E. Cousin, M.I. Schmidt, K.L. Ong, et al. Burden of diabetes and hyperglycaemia in adults in the Americas, 1990–2019: a systematic analysis for the global burden of disease study 2019, Lancet Diabetes Endocrinol. 10 (2022), 655–667. https://doi.org/10.1016/S2213-8587(22)00186-3.

[4] S. Chatterjee, K. Khunti, M.J. Davies, Type 2 diabetes, The Lancet 389 (2017), 2239–2251. https://doi.org/10.1016/S0140-6736(17)30058-2.

[5] P. Saeedi, I. Petersohn, P. Salpea, et al. Global and regional diabetes prevalence estimates for 2019 and projections for 2030 and 2045: results from the international diabetes federation diabetes atlas, 9th edition, Diabetes Res. Clin. Pract. 157 (2019), 107843. https://doi.org/10.1016/j.diabres.2019.107843.

[6] J. Harreiter, A. Kautzky-Willer, Sex and gender differences in prevention of type 2 diabetes, Front. Endocrinol. 9 (2018), 220. https://doi.org/10.3389/fendo.2018.00220.

[7] M.A.B. Khan, M.J. Hashim, J.K. King, et al. Epidemiology of type 2 diabetes – global burden of disease and forecasted trends, J. Epidemiol. Glob. Health 10 (2019), 107. https://doi.org/10.2991/jegh.k.191028.001.

[8] A. Kautzky-Willer, J. Harreiter, G. Pacini, Sex and gender differences in risk, pathophysiology and complications of type 2 diabetes mellitus, Endocr. Rev. 37 (2016), 278–316. https://doi.org/10.1210/er.2015-1137.

[9] A.G. Huebschmann, R.R. Huxley, W.M. Kohrt, et al. Sex differences in the burden of type 2 diabetes and cardiovascular risk across the life course, Diabetologia 62 (2019), 1761–1772. https://doi.org/10.1007/s00125-019-4939-5.

[10] D. Aune, T. Norat, M. Leitzmann, et al. Physical activity and the risk of type 2 diabetes: a systematic review and dose–response meta-analysis, Eur. J. Epidemiol. 30 (2015), 529–542. https://doi.org/10.1007/s10654-015-0056-z.

[11] E.A. Hernandez-Vargas, J.X. Velasco-Hernandez, In-host mathematical modelling of COVID-19 in humans, Ann. Rev. Control 50 (2020), 448–456. https://doi.org/10.1016/j.arcontrol.2020.09.006.

[12] O.I. Idisi, T.T. Yusuf, A mathematical model for lassa fever transmission dynamics with impacts of control measures: analysis and simulation, Eur. J. Math. Stat. 2 (2021), 19–28. https://doi.org/10.24018/ejmath.2021.2.2.17.

[13] M. D'Arienzo, A. Coniglio, Assessment of the Sars-Cov-2 basic reproduction number, R_0, based on the early phase of COVID-19 outbreak in Italy, Biosafe. Health 2 (2020), 57–59. https://doi.org/10.1016/j.bsheal.2020.03.004.

[14] I. Cooper, A. Mondal, C.G. Antonopoulos, A SIR model assumption for the spread of COVID-19 in different communities, Chaos Solitons Fractals, 139 (2020), 110057. https://doi.org/10.1016/j.chaos.2020.110057.

[15] S. Rezapour, H. Mohammadi, A. Jajarmi, A new mathematical model for Zika virus transmission, Adv. Differ. Equ. 2020 (2020), 589. https://doi.org/10.1186/s13662-020-03044-7.

[16] F. Mrope, N. Jeeva, Modeling the transmission dynamics of banana bunch top disease in banana plants, Eurasian J. Math. Computer Appl. 12 (2024), 73–90. https://doi.org/10.32523/2306-6172-2024-12-3-73-90.

[17] A. Ferdous, An ordinary differential equation model for assessing the impact of lifestyle intervention on type 2 diabetes epidemic, Healthc. Anal. 4 (2023), 100271. https://doi.org/10.1016/j.health.2023.100271.

[18] L. Ebiwareme, F.A.P. Kormane, E.O. Odok, Simulation of unsteady mhd flow of incompressible fluid between two parallel plates using Laplace-Adomian decomposition method, World J. Adv. Res. Rev. 14 (2022), 136–145. https://doi.org/10.30574/wjarr.2022.14.3.0456.

[19] J. Xu, H. Khan, R. Shah, et al. The analytical analysis of nonlinear fractional-order dynamical models, AIMS Math. 6 (2021), 6201–6219. https://doi.org/10.3934/math.2021364.

[20] M. Thongmoon, S. Pusjuso, The numerical solutions of differential transform method and the laplace transform method for a system of differential equations, Nonlinear Anal.: Hybrid Syst. 4 (2010), 425–431. https://doi.org/10.1016/j.nahs.2009.10.006.

[21] A. Harir, S. Melliani, H. El Harfi, et al. Variational iteration method and differential transformation method for solving the SEIR epidemic model, Int. J. Differ. Equ. 2020 (2020), 3521936. https://doi.org/10.1155/2020/3521936.

[22] A.A. Adeniji, O.A. Mogbojuri, M.C. Kekana, et al. Numerical solution of rotavirus model using Runge-Kutta-Fehlberg method, differential transform method and Laplace Adomian decomposition method, Alexandria Eng. J. 82 (2023), 323–329. https://doi.org/10.1016/j.aej.2023.10.001.

[23] N. Jeeva, K.M. Dharmalingam, S.E. Fadugba, et al. Implementation of Laplace Adomian decomposition and differential transform methods for Sars-Cov-2 model, J. Appl. Math. Inform. 42 (2024), 945–968. https://doi.org/10.14317/JAMI.2024.945.

[24] S.E. Fadugba, M.C. Kekana, N. Jeeva et al. Development and implementation of innovative higher order inverse polynomial method for tackling physical models in epidemiology, J. Math. Computer Sci. 36 (2024), 444–454. https://doi.org/10.22436/jmcs.036.04.07.

[25] N. Jeeva, K.M. Dharmalingam., Analytical expression of HIV infection model using Taylor series method (TSM), Int. J. Creat. Res. Thoughts, 11 (2023), 859–867. https://ssrn.com/abstract=4559838.

[26] N. Jeeva, K.M. Dharmalingam., Solving non-homogeneous lane-embed equation using Taylor series method, Commun. Nonlinear Anal. 12 (2024), 1–5.

[27] N. Jeeva, K.M. Dharmalingam, Sensitivity analysis and semi-analytical solution for analyzing the dynamics of coffee berry disease, Computer Res. Model. 16 (2024), 731–753. https://doi.org/10.20537/2076-7633-2024-16-3-731-753.

[28] N. Jeeva, K.M. Dharmalingam, Mathematical analysis of new SEIQR model via Laplace Adomian decomposition method, Indian J. Nat. Sci. 15 (2024), 72148–72157.

[29] K.M. Dharmalingam, N. Jeeva, N. Ali, et al. Mathematical analysis of Zika virus transmission: exploring semi-analytical solutions and effective controls, Commun. Math. Biol. Neurosci. 2024 (2024), 112. https://doi.org/10.28919/cmbn/8719.

[30] S. Geethamalini, S. Balamuralitharan, Semianalytical solutions by homotopy analysis method for EIAV infection with stability analysis, Adv. Differ. Equ. 2018 (2018), 356. https://doi.org/10.1186/s13662-018-1808-3.

[31] G. Suganya, R. Senthamarai, Analytical approximation of a nonlinear model for pest control in coconut trees by the homotopy analysis method, Computer Res. Model. 14 (2022), 1093–1106. https://doi.org/10.20537/2076-7633-2022-14-5-1093-1106.

[32] M. Ali, N. Anjum, Q.T. Ain, et al. Homotopy perturbation method for the attachment oscillator arising in nanotechnology, Fibers Polymers 22 (2021), 1601–1606. https://doi.org/10.1007/s12221-021-0844-x.

[33] S. Balamuralitharan, S. Vigneshwari, Solutions of viral dynamics in hepatitis b virus infection using hpm, in: S. Smys, A.M. Iliyasu, R. Bestak, F. Shi (Eds.), New Trends in Computational Vision and Bio-Inspired Computing, Springer, Cham, 2020: pp. 451–461. https://doi.org/10.1007/978-3-030-41862-5_43.

[34] R.T. Abah, A.B. Zhiri, K. Oshinubi, A. Adeniji, Mathematical analysis and simulation of ebola virus disease spread incorporating mitigation measures, Franklin Open 6 (2024), 100066. https://doi.org/10.1016/j.fraope.2023.100066.